Supporting Information

Walter et al. 10.1073/pnas.1116315109

SI Methods

Isolation and Purification of Cytoplasmic Dynein. Native, double-headed dynein was isolated largely as described by Toba and Toyoshima (1). Four fresh porcine brains (450 g) were homogenized in 450 mL of PMEE (35 mM Pipes-KOH, pH 7.2, 5 mM $MgSO_4$, 1 mM EGTA, 0.5 mM EDTA) using a hand-held blender. The homogenate was centrifuged at 9,000 rpm for 30 min in a Kontron A6.9 rotor. The supernatant was then centrifuged at 120,000 × *g* for 30 min in a Beckman 70Ti rotor. The high-speed supernatant was loaded onto a SP-Sepharose Fast Flow column (45-mL bed volume) at a flow rate of 6 mL/ min. The column was washed with approximately 100 mL of PMEE buffer before eluting with PMEE plus 0.5 M KCl. The elution peak was divided into 12-mL fractions which were layered onto 24 mL of 10–40% linear sucrose gradients and centrifuged at 100,000 × *g* for 18 h in a Beckman SW28 rotor. The sucrose gradients were fractionated into 1.5-mL fractions. Dynein-enriched fractions, as determined by SDS–PAGE (2), were filtered through 0.45 μm PTFE syringe-tip filters (Millipore, Bedford, MA) and loaded onto a Resource Q column (Pharmacia) at 0.5 mL/ min flow rate using an FPLC system (Pharmacia). The column was washed with 5 mL of PMEE containing 10% sucrose, 0.01 mM ATP, and 90 mM KCl. The dynein was eluted from the column with PMEE buffer containing 10% sucrose, 0.01 mM ATP, and 140 mM KCl. The dynein fractions with the highest purity were mixed with an equal volume of PMEE containing 2 M sucrose, frozen in liquid nitrogen, and stored at −80 °C. The protein concentration of the dynein was determined by the method of Bradford (3). For possible kinesin contamination the purified dynein was tested by SDS-PAGE and immunoblot (Fig. S5). Before use, active dynein was purified using a microtubule binding and release step with 10 mM Mg-ATP.

Tubulin Purification and Labeling. Tubulin was isolated from fresh porcine brain by two cycles of polymerization-depolymerization in the presence of 500 mM piperazine-N,N'-bis(2-ethanesulfonic acid) (PIPES) buffer as described by Castoldi and Popov (4). Some tubulin was purified additionally by phosphocellulose column chromatography. The purity of the tubulin was determined by SDS-PAGE (Fig. S5). Aliquots were frozen in liquid nitrogen and stored at 80 °C. Biotin-labeled and rhodamine-labeled tubulins were prepared following protocols of the Mitchison laboratory (5).

Optical Trap Experiments. Optical trap experiments were carried out in 35 mM PIPES (pH 7.4), 1 mM EGTA, and an ATP regeneration system (10 mM creatine-phosphate, 10 U/mL creatine kinase) and a deoxygenating system (10 mg/mL glucose, 15 U/mL glucose oxidase, 30 μg/mL catalase, 10 mM DTT). The concentrations of Mg-ATP, KH_2PO_4 (Pi) and Mg^{2+} were varied as indicated. The contamination of creatine-phosphate with free Pi was analyzed using the EnzChek Phosphate Assay Kit from Molecular Probes (9) and found to be approximately 25 μM per 10 mM creatine-phosphate (Table S1). The cover slip of a microscope flow chamber was coated with a thin layer of nitrocellulose containing 1.5 μm glass beads. The flow chamber was then incubated for 1 min with approximately 1 μg/mL dynein and subsequently washed several times to remove excess dynein and free ATP.

To distinguish polarity of the microtubule dumbbell and to improve compliance of the microtubule-bead link, the minus-end of a microtubule (MT) was attached end-on to a 1 μm latex microsphere (bead) using an antibody specific for the minus-end of α-tubulin. To generate a minus-end specific antibody we designed two peptides (1tub, aa31–40, aa242–252) according to Fan, et al. (6) and Nogales, et al. (7), linked them to keyhole Limpet protein, and used them as antigens to immunize rabbits. The antibodies were purified by protein-G column chromatography and linked to carboxylated latex beads using 1-Ethyl-3-(3-dimethylaminopropyl) carbodiimide as cross-linker. A slightly smaller bead (0.8 μm) was attached laterally near the MT plus-end using the avidin/biotin chemistry as has been described for actin-bead dumbbells (8). Each bead was held in a weak optical trap. The dumbbell was positioned over a dynein molecule, which was attached nonspecifically to the top surface of a 1.5 μm glass bead immobilized on a microscope cover slip. To ensure MT-dynein interactions were from a single molecule, the microscopic flow chambers were sparsely coated with dynein such that events were found only on one out of 3–5 glass beads. Experiments were performed with a custom-built optical trap based on a Nikon TE2000 microscope using a four Watt 1064-nm laser (Coherent GmbH, 23569 Lübeck, Germany) and a 1.49 NA TIRF objective lens from Nikon. Bead positions were detected by a four-quadrant photo diode detector, sampled at 10 kHz, and filtered at 5 kHz. Binding events were detected by a reduction (>2*x*) in the variance of the bead position. Only those binding events with a minimal life time of 20 ms were used to determined the apparent working stroke. Trap stiffness was calculated from the Brownian noise of the bead position. To achieve relatively high link stiffness between latex beads and MT we stretched the dumbbell by moving the trapped beads apart at a laser power giving a trap stiffness of about 0.1 to 0.2 pN/nm. The total stiffness along the *x*-axis of the free dumbbell was then reduced by using a positive feedback system in alternating current (AC) mode as previously described (8).

The link stiffness of the MT-bead attachment was determined from autovariance records of each bead and the covariance record, constructed form the position records using a program developed by David Smith (10). The link stiffness of the MT end-on attachment of the bead was in the range of 1–2 pN/nm whereas the link stiffness of the lateral attachments was in the range of 0.2–0.3 pN/nm. Only data obtained from the beads with end-on attachment were used to determine the working stroke of dynein. No compliance correction was required because of the high link stiffness.

Gliding Assays. Bead-MT complexes as used for the dumbbell assay were added to a flow chamber that was precoated with 40 μg/mL of full-length dimeric rat kinesin-1 expressed in *Escherichia coli*. Gliding was measured in 35 mM PIPES (pH 7.4), 1 mM EGTA, 1 mM ATP, an ATP regeneration system, and a deoxygenating system. Out of 76 measured complexes 74 had the expected orientation; i.e. the MT minus-end was attached to the bead. In this orientation the bead is attached to the leading end in a kinesin-based gliding assay (Movie S1). A bead attachment to the trailing end of the MT was observed in two cases only.

Some MT gliding assays were carried out using polarity-marked MTs. To produce polarity-marked MTs Guanosine-5'-[(α,β)-methyleno]triphosphate (GMPCPP)-stabilized Alexa488-labeled MTs were incubated in BRB80 with 0.6 μM rhodamine-labeled tubulin in the presence of 14 μM N-ethylmaleimide and 1 mM GMPCPP. A dichlorodimethylsilane-coated (Sigma-Aldrich) flow chamber was incubated with 50 μg/mL antidynein

intermediate chain (MAB1614, Millipore). The surface was blocked with 1% Pluronic F-127 (Molecular Probes) in BRB80. Cytoplasmic dynein was bound to the antibody at 20 μg/mL. The gliding assay was then performed with the polarity-marked MTs under buffer conditions identical to the dumbbell assay with 1 μM ATP and no or 1 mM Pi respectively (Movies S2 and 3).

1. Toba S, Toyoshima Y (2004) Dissociation of double-headed cytoplasmic dynein into single-headed species and its motile properties. *Cell Motil Cytoskeleton* 58:281–289.
2. Laemmli UK (1970) Cleavage of structural proteins during the assembly of the head of bacteriophage T4. *Nature* 227:680–685.
3. Bradford MM (1976) A rapid and sensitive method for the quantification of microgram quantities of protein utilizing the principle of protein-dye binding. *Anal Biochem* 151:369–374.
4. Castoldi M, Popov AV (2003) Purification of brain tubulin through two cycles of polymerization-depolymerization in a high-molarity buffer. *Protein Expr Purif* 32:83–88.
5. Hyman A, et al. (1991) Preparation of modified tubulins. *Methods Enzymol* 196:478–485.
6. Fan J, Griffiths AD, Lockhart A, Cross RA, Amos LA (1996) Microtubule minus ends can be labeled with a phage display antibody specific to alpha-tubulin. *J Mol Biol* 259:325–330.
7. Nogales E, Wolf SG, Downing KH (1998) Structure of the alpha beta tubulin dimer by electron crystallography. *Nature* 391:199–203.
8. Steffen W, Smith D, Simmons R, Sleep J (2001) Mapping the actin filament with myosin. *Proc Natl Acad Sci USA* 98:14949–14954.
9. Webb MR (1992) A continuous spectrophotometric assay for inorganic phosphate and for measuring phosphate release kinetics in biological systems. *Proc Natl Acad Sci USA* 89:4884–4887.
10. Smith DA, Steffen W, Simmons RM, Sleep J (2001) Hidden-Markov methods for the analysis of single-molecule actomyosin displacement data: the variance-hidden-markov method. *Biophys J* 81:2795–2816.

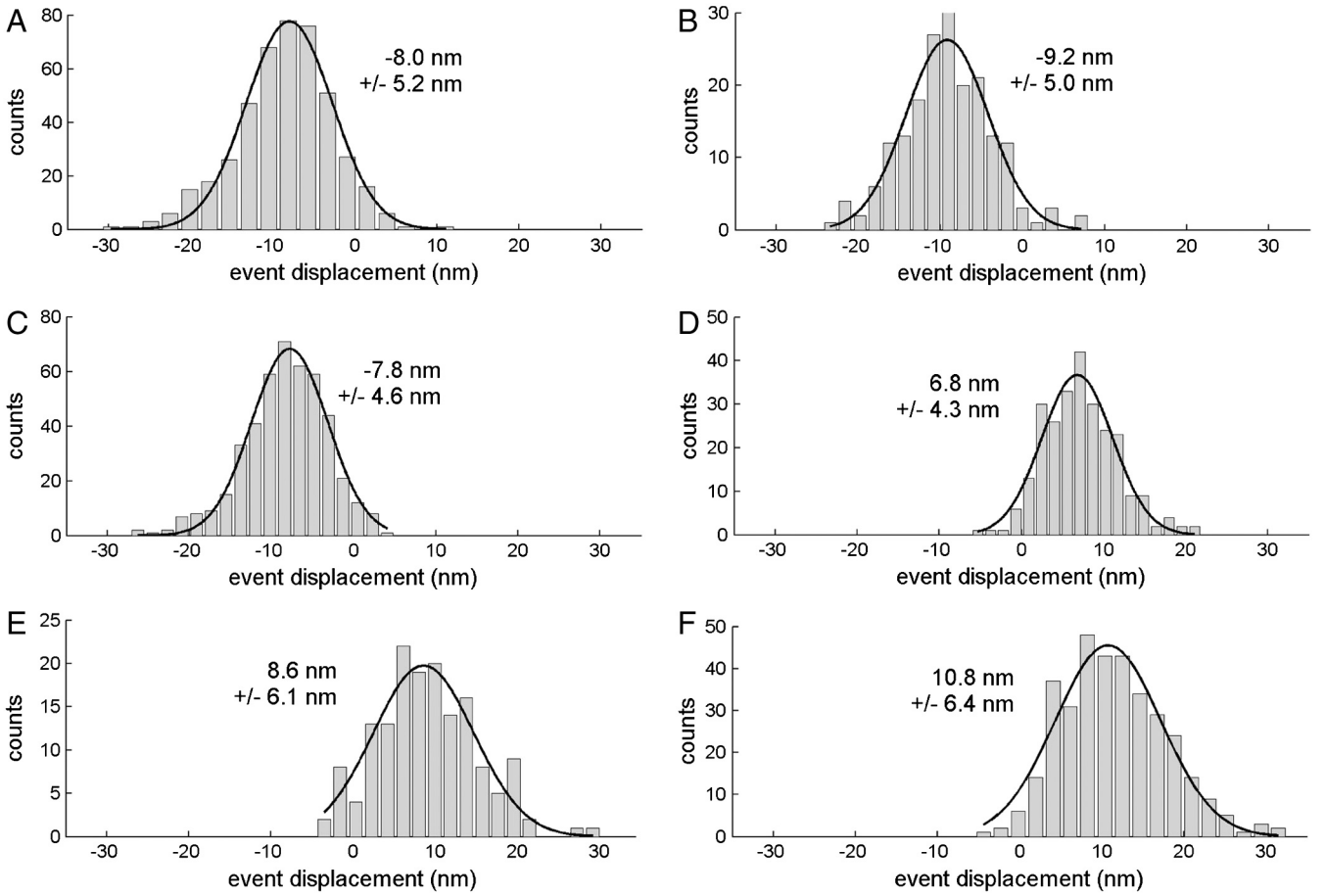

Fig. S1. Example histograms of binding events of single motors at 0 mM (*A*, *B*), 0.3 mM (*C*, *D*), and 1 mM (*E*, *F*) phosphate. The working stroke was calculated by a Gaussian fit of the distribution of the binding events. The result of each Gaussian fit is represented as one data point in Fig. 3. At 0 mM phosphate the motors perform a working stroke towards the MT minus-end (*A*, *B*), at 1 mM phosphate towards the plus-end (*E*, *F*), and at 0.3 mM phosphate either toward the plus-end or the minus-end (*C*, *D*).

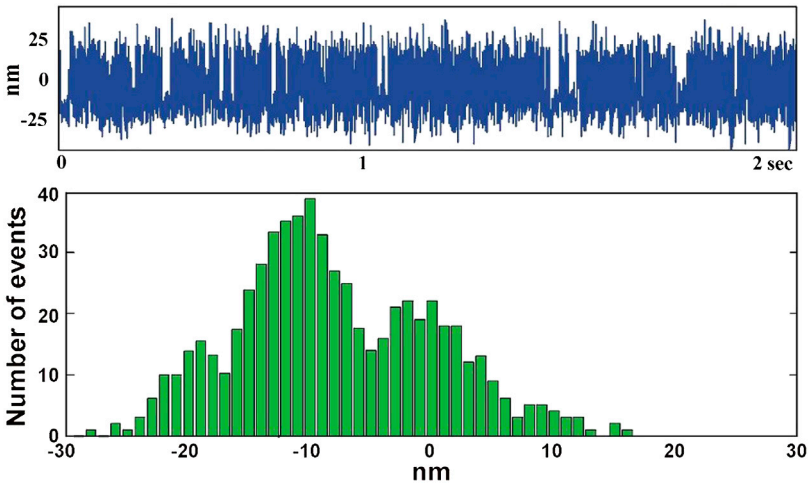

Fig. S2. Detection of the 8 nm spacing of the dynein binding sites on a MT. The glass bead with its attached motor protein was held stationary by employing a XYZ piezo-controled feedback loop as described earlier [Steffen et al. (8)]. Data were collected with the optical trap setup described by [Steffen et al. (8)]. Experiments were performed with 10 μM Mg-ATP in 25 mM Hepes buffer, pH 7.4 containing 25 mM KCl, 4 mM $MgCl_2$, and an antibleach system (10 mg/mL glucose, 15 U/mL glucose oxidase, 30 μg/mL catalase, 10 mM DTT).

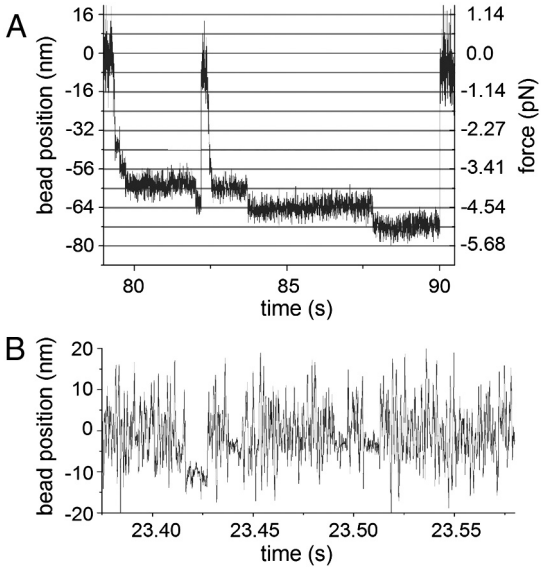

Fig. S3. Influence of [Mg^{2+}] and [ATP] on the processive movement of cytoplasmic dynein. (*A*) At 1 mM Mg^{2+} and 0.1 mM Mg-ATP cytoplasmic dynein moved processively along the MT; however, processivity was abolished when Mg^{2+} concentration was raised to 10 mM but keeping the Mg-ATP concentration constant (*B*). All experiments were carried out at low ionic strength (35 mM Pipes-KOH).

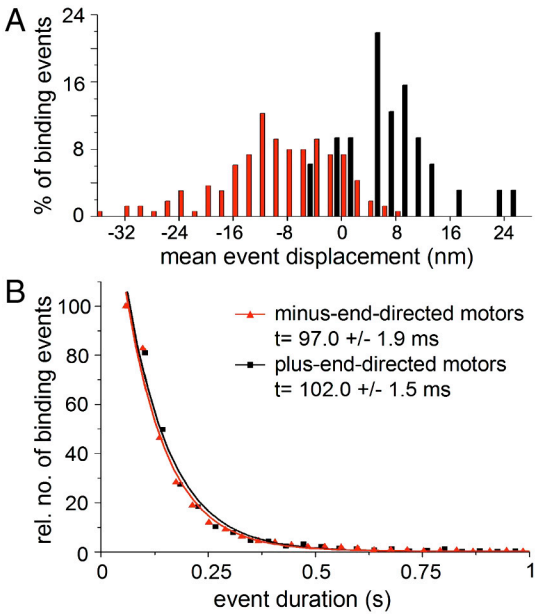

Fig. S4. Influence of phosphate on the directionality of the apparent working stroke of dynein. (*A*) At 1 μM Mg-ATP, 1 mM Mg^{2+}, and 0.3 mM phosphate two dyneins could be recorded using the *same* MT dumbbell, one motor producing an apparent working stroke of approximately −8 nm and the other motor an apparent working stroke of approximately +8 nm. (*B*) Lifetimes distributions of binding events of minus-end-directed (0–0.2 mM Pi) and plus-end-directed (0.5–1 mM Pi) cytoplasmic dynein at 1 μM Mg-ATP and 1 mM Mg^{2+} were nearly identical.

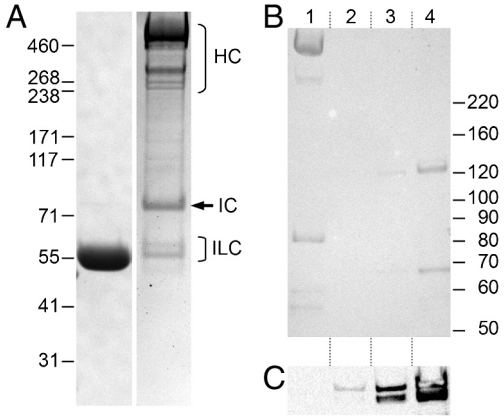

Fig. S5. Determination of the purity of cytoplasmic dynein. (*A*) SDS-PAGE of purified tubulin (left lane) and cytoplasmic dynein (right lane). The bands show the heavy chain (HC), intermediate chain (IC), and intermediate light chains (ILC). There is no band with the size of kinesin-1 (131 kDa). (*B*) Ponceau-stained membrane and (*C*) immunoblot of 2 μg dynein (lane 1) and 50 ng (lane 2), 200 ng (lane 3), or 500 ng (lane 4) porcine kinesin-1. There was no detectable kinesin-1 contamination in the purified dynein (*B*) or the purified tubulin [(*A*), left lane].

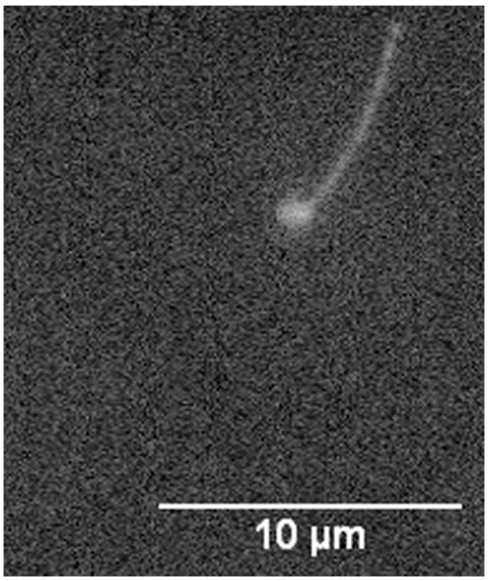

Movie S1. Movement of bead-MT complex over a kinesin coated surface. The MT was attached to the bead surface via an antibody specific to the MT minus-end.

Movie S1 (AVI)

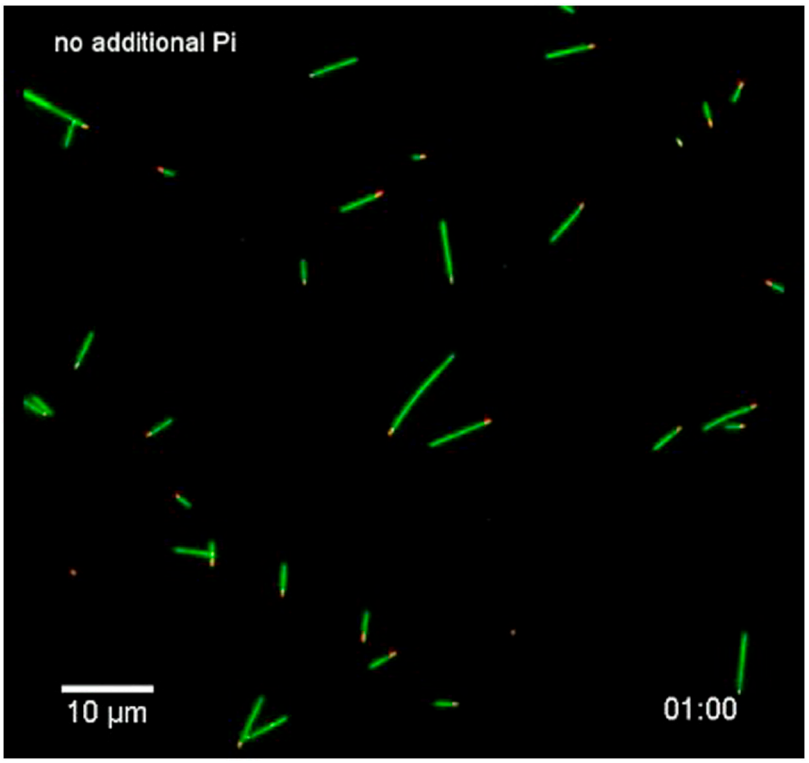

Movie S2. Cytoplasmic dynein-dependent MT gliding in absence of phosphate. To investigate whether a change in the directionality of movement could also be achieve for an ensemble of dynein motors, a MT gliding assay was performed. The same conditions have been used as described for the single molecule optical trap experiments (35 mM Pipes, pH 7.4, 1 mM EGTA, 1 mM $MgCl_2$, 1 µM Mg-ATP). Time 00:00 min:s (time lapse).

Movie S2 (AVI)

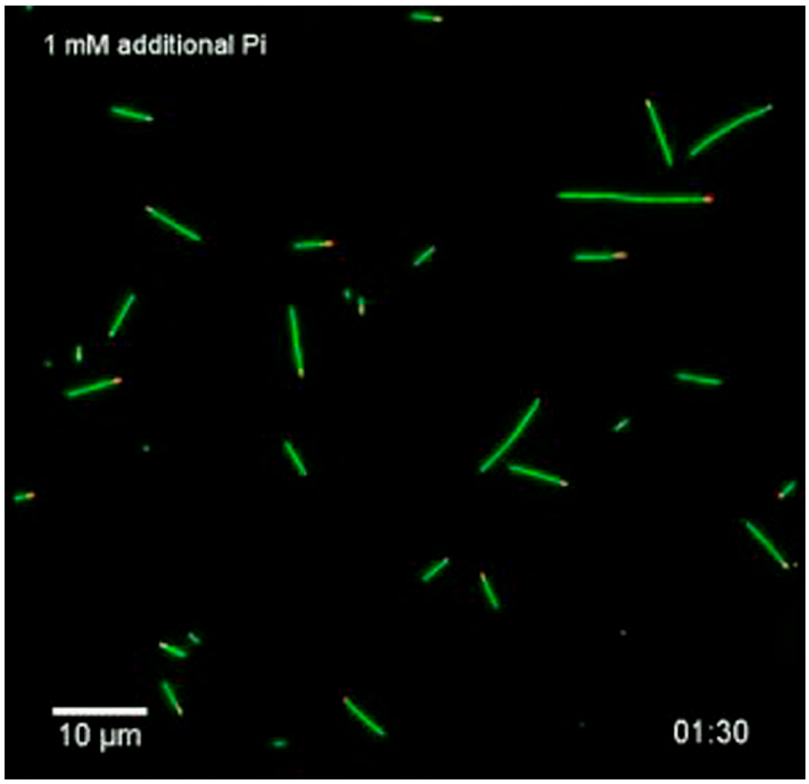

Movie S3. Cytoplasmic dynein-dependent MT gliding in presence (S3) of phosphate. To investigate whether a change in the directionality of movement could also be achieve for an ensemble of dynein motors, a MT gliding assay was performed. The same conditions have been used as described for the single molecule optical trap experiments (35 mM Pipes, pH 7.4, 1 mM EGTA, 1 mM $MgCl_2$, 1 μM Mg-ATP, and 1 mM Pi). Time 00:00 min:s (time lapse).

Movie S3 (AVI)

Table S1. Determination of the concentration of free Pi in buffer system (*35 mM Pipes, pH 7.4, 1 mM EGTA, 1 mM $MgCl_2$, 1 mM DTT)

buffer	[free Pi]
BRB35*	0.027 mM ± 0.025
BRB35 plus 1 mM Pi	1.054 mM ± 0.065
BRB35 plus 3 mM $MgCl_2$ and 1 mM Pi	1.083 mM ± 0.062
10 mM creatine-phosphate	0.024 mM ± 0.002